

# Fundamental limits on determination of photon number statistics from measurements with multiplexed on/off detectors

Jaromír Fiurášek

*Department of Optics, Faculty of Science, Palacký University,  
17. listopadu 12, 77900 Olomouc, Czech Republic*

We investigate fundamental bounds on the ability to determine photon number distribution and other related quantities from tomographically incomplete measurements with an array of  $M$  detectors that can only distinguish the absence or presence of photons. We show that the lower and upper bounds on photon number probabilities can be determined by solving a linear program. We present and discuss numerical results for various input states including thermal states, coherent states, squeezed states, and highly non-classical single-photon subtracted squeezed vacuum states. Besides photon number probabilities we also investigate bounds on the parity of photon number distribution which determines the value of Wigner function of the state at the origin of phase space. Moreover, we also discuss estimation of mean photon number as an example of a quantity described by an unbounded operator. Our approach and results can provide quantitative guidance on the number of detection channels required to determine the photon number distribution with a given precision.

## I. INTRODUCTION

Experimental determination of photon number distribution is a long studied problem in quantum optics. Besides being of fundamental interest, the detection and counting of photons represents an important ingredient of many protocols and schemes in optical quantum information processing and quantum metrology. As the technology progresses, detectors that can directly count the number of photons have become available [1–7]. Nevertheless, many commonly employed detectors can only distinguish the presence and absence of photons. Approximate photon-number resolving detectors can be constructed from such binary on/off detectors by spatial or temporal multiplexing [8]. The signal is split into  $M$  modes and sent onto an array of  $M$  detectors, and the number of detector clicks provides information about the photon number distribution. Such multiplexed photon detectors have been thoroughly investigated and utilized in numerous experiments [9–31].

Since the number of detection channels  $M$  is finite, the click statistics measured by the multiplexed detector generally does not fully and uniquely specify the photon number distribution. In other words, infinitely many different photon number distributions can yield the same click statistics. One can attempt to remove this ambiguity by making some additional assumptions, e.g. that the photon number distribution has the maximum entropy compatible with the observed click statistics [25]. However, such additional assumptions may not be generally justified, especially if the goal is to characterize artificially generated quantum states with non-trivial photon number distributions.

In the present work, we avoid such additional assumptions and we investigate the resulting fundamental uncertainty of determination of the photon number distribution from the measured click statistics. The click statistics allows us to obtain lower and upper bounds on the

photon number probabilities  $p_n$  as well as on other quantities that can be expressed as linear combinations of  $p_n$ . We show that these lower and upper bounds can be determined by solving a suitably formulated linear program. We investigate the behavior of these bounds for photon number probabilities  $p_n$  and photon number parity operator, which specifies the value of the Wigner function of the state at the origin of phase space.

For a given fixed photon number distribution the estimation precision increases with the increasing number of detection channels  $M$  and also increases with increasing detection efficiency  $\eta$ . Such behavior is certainly not surprising, but our approach allows us to precisely quantify the impact of  $M$  and  $\eta$  on the uncertainty of determination of  $p_n$ . As each detector and detection channel represents a valuable resource, our analysis can be used to identify the minimum number of detection channels  $M$  to achieve the required measurement and estimation precision.

We also investigate the determination of the mean photon number  $\bar{n}$ . Since the photon number operator is unbounded, the click statistics generally does not yield a finite upper bound on  $\bar{n}$ . However, we show that by making some minimal assumptions about the maximum photon number that can non-negligibly contribute to  $\bar{n}$ , useful estimates of  $\bar{n}$  can be obtained even for moderate number of detection channels  $M$ . We complement our numerical analysis by examples of simple analytical bounds on the single photon probability  $p_1$  and the two-mode probability  $p_{1,1}$  that a single photon is present in each mode.

The rest of the paper is organized as follows. In Section II we describe the considered measurement scheme and formulate the linear program that is used to obtain the fundamental bounds on photon number probabilities  $p_n$  and other related quantities. Numerical results are presented and discussed in Section III. Determination of mean photon number from click statistics is analyzed within our framework in Section IV. Examples of

simple analytical bounds on probabilities  $p_1$  and  $p_{1,1}$  are given in Section V. Finally, Section VI contains a brief discussion and conclusions.

## II. MEASUREMENT SCHEME

The considered measurement scheme is depicted in Fig. 1. The measured optical beam is evenly split into  $M$  channels and each channel is measured with a binary detector that can distinguish the presence and absence of photons. The measured click statistics  $c_m$  represent probabilities that exactly  $m$  detectors click simultaneously. Assuming total detection efficiency  $\eta$  to be the same for each detector, the click statistics is determined by the photon number distribution  $p_n$  of the measured optical beam as follows,

$$c_m = \sum_{n=m}^{\infty} C_{mn} p_n, \quad (1)$$

where [25]

$$C_{mn} = \binom{M}{m} \sum_{j=0}^m (-1)^j \binom{m}{j} \left[ 1 - \eta + \frac{(m-j)\eta}{M} \right]^n. \quad (2)$$

Sampling of the click statistics (1) is equivalent to measurement of probabilities of projection onto vacuum  $q_{0,k}$  of the input state transmitted through lossy channels with transmittances  $T_k = \eta k/M$ ,  $0 \leq k \leq M$  [32]

$$q_{0,k} = \sum_{n=0}^{\infty} (1 - T_k)^n p_n. \quad (3)$$

It holds that

$$c_m = \binom{M}{m} \sum_{j=0}^m (-1)^j \binom{m}{j} q_{0,M-m+j}. \quad (4)$$

This implies that instead of the spatially multiplexed scheme in Fig. 1 one could also in principle utilize a scheme that includes only a single on/off detector and the transmittance  $T_k$  is set by tunable attenuator [32, 33]. By performing measurements for various  $T_k$ , the probabilities  $q_{0,k}$  can be sampled and the click statistics  $c_m$  recovered from Eq. (4).

Measurement with the multiplexed detector yields  $M$  independent parameters. This means that the measurement is tomographically incomplete and the probabilities  $p_n$  cannot be fully unambiguously reconstructed from the click statistics  $c_m$ . Many different distributions  $p_n$  can yield exactly the same click statistics  $c_m$  and are therefore fundamentally indistinguishable by the measurement. The measurement data nevertheless restrict the region of allowed  $p_n$ . For each  $p_n$  it is possible to determine a region of allowed values  $p_n \in [p_{n,\min}, p_{n,\max}]$ .

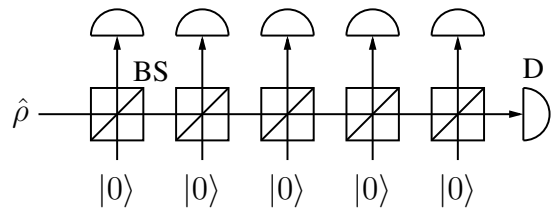


FIG. 1. Multiplexed detector of photons. The input signal is evenly split among  $M$  output modes, e.g., by an array of beam splitters with suitably chosen transmittances. Each output mode is measured with a binary detector  $D$  that can distinguish the presence and absence of photons. The number of detector clicks  $m$  represents the measured signal.

Similar interval estimates can also be established for physical quantities  $Z$  that are linear functions of  $p_n$ ,

$$Z = \sum_{n=0}^{\infty} z_n p_n, \quad (5)$$

provided that the coefficients  $z_n$  are bounded and there exists finite  $B > 0$  such that  $|z_n| < B$  holds for all  $n$ .

In this work we are interested in the effect of finite number of detection channels. We will therefore assume that the true values of  $c_m$  (or, equivalently,  $q_{0,k}$ ) are known. In most cases we shall assume  $\eta = 1$  but the presented methods can be straightforwardly extended to imperfect detectors with  $\eta < 1$ . We provide below explicit examples illustrating the effect of  $\eta$  on determination of  $p_n$ .

In order to determine the maximum and minimum values of  $Z$  compatible with the observed click statistics, we should maximize or minimize  $Z$  under the equality constraints given by Eq. (1) or equivalently by Eq. (3), and the additional constraints

$$p_n \geq 0, \quad \sum_{n=0}^{\infty} p_n = 1. \quad (6)$$

This is an instance of a linear program. We can write all the equality constraints in general form as

$$b_k = \sum_{n=0}^{\infty} A_{kn} p_n. \quad (7)$$

Since  $n$  is unbounded, we must truncate the photon number distribution at some finite cut-off  $N$  when performing the calculations. Assuming that we know the true photon number distribution  $p_{n,\text{true}}$  we can formulate a linear program for a finite vector  $\vec{x} = (x_0, \dots, x_N)$ :

$$\begin{aligned} & \text{minimize} \quad \tilde{Z} = \sum_{n=0}^N z_n x_n, \\ & \text{under the constraints} \\ & x_n \geq 0, \quad 0 \leq n \leq N, \\ & \tilde{b}_k = \sum_{n=0}^N A_{kn} x_n, \quad 0 \leq k \leq M, \end{aligned} \quad (8)$$

where

$$\tilde{b}_k = \sum_{n=0}^N A_{kn} p_{n,\text{true}}. \quad (9)$$

The advantage of this approach is that the linear program (8) is feasible by construction, because the vector  $x_n = p_{n,\text{true}}$ ,  $0 \leq n \leq N$ , obviously satisfies all the constraints. In order to account for the tail of the true distribution, the lower and upper bounds corresponding to optimization over  $p_n$  up to  $n = N$  can be calculated as

$$Z_{\min} = \tilde{Z}_{\min} + \delta Z, \quad Z_{\max} = \tilde{Z}_{\max} + \delta Z, \quad (10)$$

where

$$\delta Z = \sum_{n=N+1}^{\infty} z_n p_{n,\text{true}}. \quad (11)$$

Maximum and minimum values of  $p_m$  can be obtained by choosing  $z_n = \pm \delta_{mn}$  and the tail  $\delta Z$  vanishes in this case. The true lower and upper bounds are obtained in the limit  $N \rightarrow \infty$ . In practice, it is sufficient to choose  $N$  large enough such that  $\sum_{n=N+1}^{\infty} p_{n,\text{true}}$  becomes negligibly small. Examples of dependence of the lower and upper bounds on  $N$  are given below.

Optimality of the solution of the linear program (8) can be verified by solving the corresponding dual program

$$\begin{aligned} & \text{maximize} \quad \tilde{Y} = \sum_{k=0}^M y_k \tilde{b}_k, \\ & \text{under the constraints} \quad (12) \\ & \sum_{k=0}^M y_k A_{kn} \leq z_n, \quad 0 \leq n \leq N. \end{aligned}$$

Any feasible solution  $\tilde{Y}$  of the dual program (12) provides a lower bound on the solution of the primal program,  $\tilde{Z}_{\min} \geq \tilde{Y}$ . Strong duality implies that equality holds for the optimal solutions,  $\tilde{Y}_{\text{opt}} = \tilde{Z}_{\text{opt}}$ . Since  $\tilde{Y}_{\text{opt}}$  is also a lower bound on  $\tilde{Z}_{\text{opt}}$ , this proves the optimality of the solution.

### III. NUMERICAL RESULTS

We have performed numerical calculations for four different types of quantum states: thermal states with Bose-Einstein photon number distribution,

$$p_{n,\text{thermal}} = \frac{1}{\bar{n} + 1} \left( \frac{\bar{n}}{\bar{n} + 1} \right)^n, \quad (13)$$

coherent states with Poisson photon number distribution,

$$p_{n,\text{coh}} = \frac{\bar{n}^n}{n!} e^{-\bar{n}}, \quad (14)$$

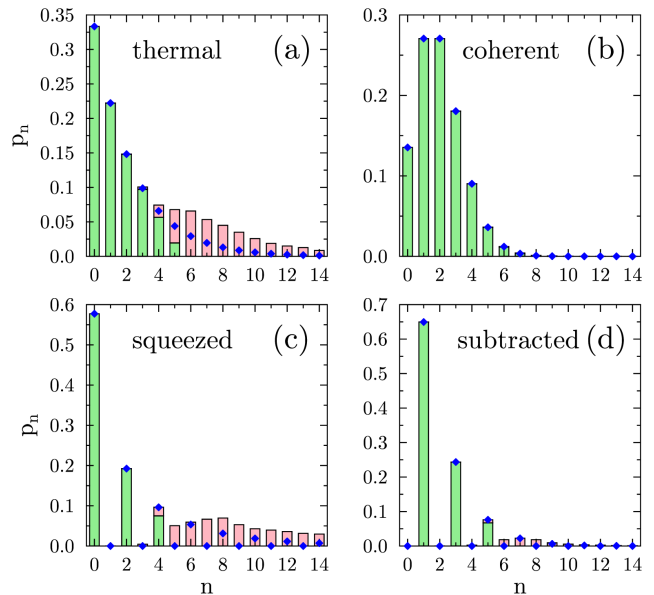


FIG. 2. Lower bounds (green bars) and upper bounds (pink bars) on the photon number probabilities  $p_n$  are plotted for four different states with  $\bar{n} = 2$ : thermal state (a), coherent state (b), squeezed vacuum state (c), and single-photon subtracted squeezed vacuum state (d). Blue diamonds indicate the true photon number distributions. Parameters of the multiplex detector read  $M = 10$  and  $\eta = 1$ , and the photon number cut-off was set to  $N = 80$  in the numerical calculations.

squeezed vacuum states that exhibit oscillations in  $p_n$ ,

$$p_{2n} = \frac{(2n)!}{2^{2n} n!^2} \frac{(\tanh r)^{2n}}{\cosh r}, \quad p_{2n+1} = 0, \quad (15)$$

and the single-photon subtracted squeezed vacuum state,

$$p_{2n-1} = \frac{(2n)!}{2^{2n} n!^2} \frac{2n (\tanh r)^{2n}}{\sinh^2 r \cosh r}, \quad p_{2n} = 0. \quad (16)$$

Here  $\bar{n}$  denotes the mean photon number and  $r$  is the squeezing constant. For the squeezed vacuum state (15) we have  $\bar{n} = \sinh^2 r$  and for the single-photon subtracted squeezed vacuum state we obtain  $\bar{n} = 1 + 3 \sinh^2 r$ .

The linear program (8) was solved with software Mathematica using the function LinearProgramming. Simplex method was utilized to carry out the optimization, which ensures that exact optimal solution is found which exactly satisfies all the constraints. The simplex algorithm is considerably slower than the interior point methods. Nevertheless, for the studied problems the calculations were fast enough even with the simplex algorithm.

The numerically determined lower and upper bounds on  $p_n$  are plotted in Fig. 2 for  $\bar{n} = 2$  and  $M = 10$ . The cut-off was set to  $N = 80$  which is large enough to ensure that the truncation has no effect on the reported results. We can observe that rather large uncertainties in the determination of  $p_n$  occur for the thermal state and squeezed vacuum state. These states exhibit large variances of the photon number operator  $\hat{n}$

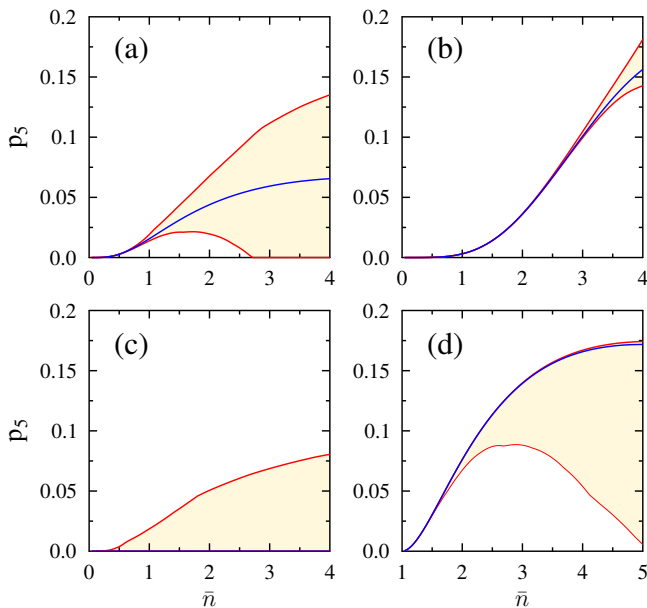


FIG. 3. Lower and upper bounds on photon number probability  $p_5$  are plotted in dependence of the mean photon number  $\bar{n}$  for four different states: thermal state (a), coherent state (b), squeezed vacuum state (c), and single-photon subtracted squeezed vacuum state (d). Blue lines indicate the true values of  $p_5$ . Parameters of the multiplexed detector read  $M = 10$  and  $\eta = 1$ .

and for the chosen mean photon number  $\bar{n}$  the population of higher Fock states with  $n > M$  is non-negligible, e.g.  $p_{11,\text{thermal}} = 0.0039$ . By contrast, the uncertainties of determination of photon number distribution of the coherent state with  $\bar{n} = 2$  is very small, because the population of Fock states above 10 is negligible, e.g.  $p_{11,\text{coh}} = 6.94 \times 10^{-6}$ . The subtraction of a photon from a squeezed vacuum state results in a narrower photon number distribution as compared to the input squeezed vacuum state, which leads to smaller uncertainties in estimation of  $p_n$ , see Fig. 2(d). Note also that the probabilities  $p_n$  of lowest photon numbers  $n$  are determined with high precision. The uncertainty

$$\Delta p_n = p_{n,\text{max}} - p_{n,\text{min}}, \quad (17)$$

first increases with  $n$  but then it starts to decrease again because having large populations of high Fock states  $|n\rangle$  with  $n \gg M$  is incompatible with the constraints imposed by  $c_m$  or equivalently by  $q_{0,k}$ .

To further illustrate the dependence of  $\Delta p_n$  on the width of the photon number distribution and the number of the detection channels, we plot in Fig. 3 the dependence of the lower and upper bounds  $p_{5,\text{min}}$  and  $p_{5,\text{max}}$  as functions of the mean photon number  $\bar{n}$  for the four considered photon number distributions. As expected, for fixed number of detection channels  $M$  the uncertainty increases with increasing width of the distribution, here quantified by  $\bar{n}$ . Figure 4 shows the dependence of the uncertainties  $\Delta p_n$  on  $M$  for a thermal state with fixed

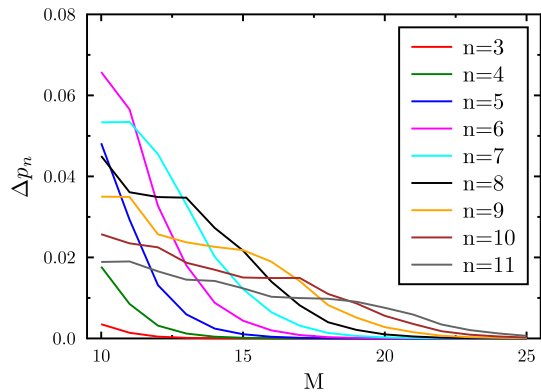


FIG. 4. The photon number uncertainties  $\Delta p_n$  are plotted as functions of the number of detector channels  $M$  for thermal state with  $\bar{n} = 2$ . Photon number cut-off is set to  $N = 80$  and  $\eta = 1$  is assumed in the numerical calculations.

photon number  $\bar{n}$ . As  $M$  increases, more information is gathered about the photon number distribution and the constraints on  $p_n$  become tighter. Consequently  $\Delta p_n$  decrease with increasing  $M$ .

The influence of detection efficiency  $\eta$  on determination of  $p_n$  is illustrated in Fig. 5. We can observe that the uncertainties  $\Delta p_n$  increase with decreasing detection efficiency, which is the expected behavior. Detection with

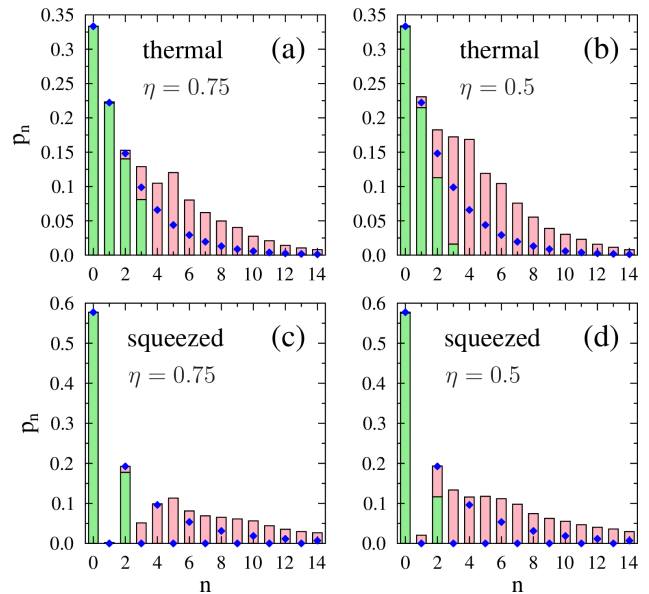


FIG. 5. Dependence of the uncertainty of determination of  $p_n$  on detection efficiency  $\eta$ . The lower bounds (green bars) and upper bounds (pink bars) on the photon number probabilities  $p_n$  are plotted for thermal state (a,b) and squeezed vacuum state (c,d) with  $\bar{n} = 2$ . Blue diamonds indicate the true photon number distributions. Parameters of the multiplexed detector read  $M = 10$ ,  $\eta = 0.75$  (a,c), and  $\eta = 0.5$  (b,d).

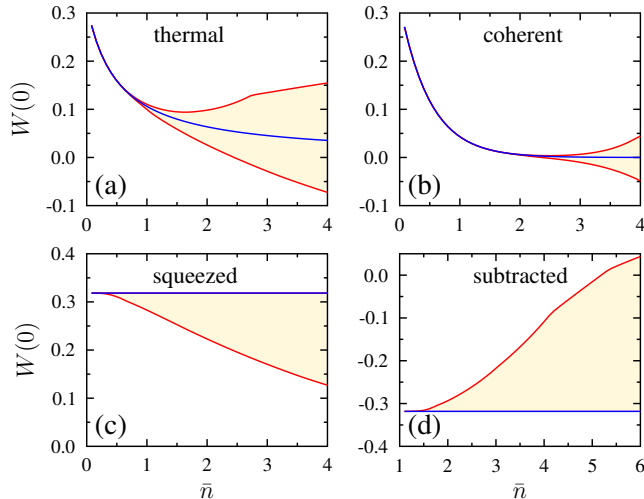


FIG. 6. Lower and upper bounds on the value of Wigner function at the origin of phase space  $W$  are plotted in dependence of the mean photon number  $\bar{n}$  for four different states: thermal state (a), coherent state (b), squeezed vacuum state (c), and single-photon subtracted squeezed vacuum state (d). Blue lines indicate the true values of  $W$ . Parameters of the detector read  $M = 10$  and  $\eta = 1$ .

efficiency  $\eta$  is equivalent to measurement with perfect detectors of a state transmitted through a lossy channel with transmittance  $\eta$ . The virtual perfect detectors then measure state with modified photon number distribution [34]

$$\tilde{p}_n = \sum_{m=n}^{\infty} \binom{m}{n} \eta^n (1-\eta)^{m-n} p_m. \quad (18)$$

On the one hand, the distribution  $\tilde{p}_n$  has reduced width with respect to the original photon number distribution  $p_n$ . For instance, for input thermal or coherent state the losses only reduce the mean photon number of the state to  $\eta\bar{n}$ . On the other hand, to recover the original distribution  $p_m$  from  $\tilde{p}_n$  one has to invert the relation (18). Overall, this results in increased uncertainties  $\Delta p_n$  for lossy detection.

As discussed above, the linear programming approach can be used to obtain the fundamental uncertainties of determination of mean value of an arbitrary bounded operator  $\hat{Z}$  diagonal in Fock basis. As an important example we consider here determination of the mean value of Wigner function at the origin of phase space,

$$W = \frac{1}{\pi} \sum_{n=0}^{\infty} (-1)^n p_n.$$

Fig. 6 shows the dependence of the numerically calculated lower and upper bounds  $W_{\min}$  and  $W_{\max}$  on the mean photon number  $\bar{n}$  for four different types of states and fixed number of detection channels  $M = 10$ . Similarly to the behavior of bounds on  $p_n$  (c.f. Fig. 3),

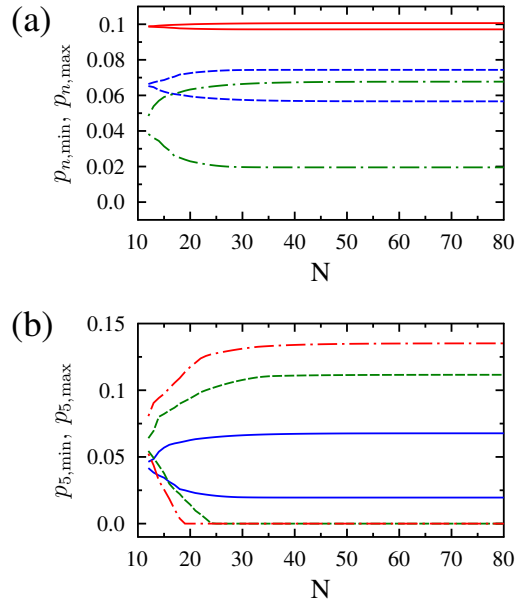


FIG. 7. Lower and upper bounds on the photon number probabilities  $p_{n,\min}$  and  $p_{n,\max}$  of thermal states are plotted in dependence on the photon number cut-off  $N$ . Parameters of the multiplexed detector read  $M = 10$  and  $\eta = 1$ . In the left panel (a) we show results for fixed  $\bar{n} = 2$  and  $n = 3$  (red solid line),  $n = 4$  (blue dashed line) and  $n = 5$  (green dot-dashed line). The right panel (b) illustrates dependence of the probability bounds on the mean photon number, with bounds on  $p_5$  plotted for  $\bar{n} = 2$  (blue solid line),  $\bar{n} = 3$  (green dashed line), and  $\bar{n} = 4$  (red dot-dashed line).

the width of the uncertainty window increases with increasing  $\bar{n}$ . For the photon-subtracted squeezed vacuum state, the considered detection scheme with ten detection channels enables unambiguous certification of negativity of Wigner function up to  $\bar{n} \approx 5.15$ . For higher mean photon numbers, the click statistics becomes compatible also with states that have positive Wigner function at the origin of phase space. The squeezed vacuum state and the single-photon subtracted squeezed vacuum state are states with well defined parity of photon number distribution. Therefore, the upper (or lower) bound on  $W$  coincides with the true value of  $W$  in those two cases.

The dependence of the numerically calculated lower and upper bounds  $p_{n,\min}$  and  $p_{n,\max}$  on the photon number cut-off  $N$  is illustrated in Fig. 7. Initially, the uncertainty window  $\Delta p_n$  increases with increasing  $N$  because more and more degrees of freedom become available for optimization. For large  $N$  the numerically calculated values saturate and converge to their true values. For the range of state parameters considered in the present work the choice  $N = 80$  turns out to be sufficient to obtain reliable results. Similar convergence behavior is observed also for other bounded quantities, such  $W$ . However, this picture changes when unbounded operators are considered and we discuss this in the following section.

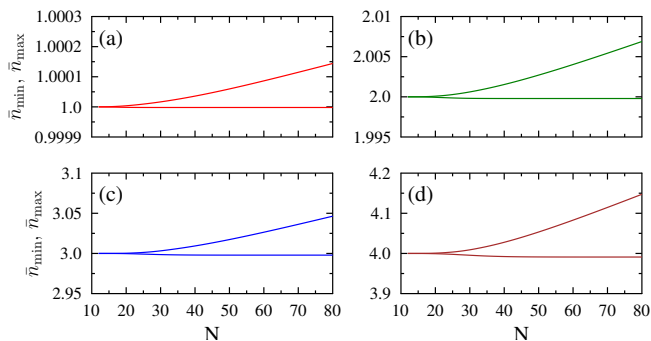


FIG. 8. The lower and upper bounds on the mean photon number  $\bar{n}_{\min}$  and  $\bar{n}_{\max}$  are plotted in dependence on the photon number cut-off  $N$ . The results are shown for thermal state with true mean photon numbers  $\bar{n} = 1$  (a),  $\bar{n} = 2$  (b),  $\bar{n} = 3$  (c), and  $\bar{n} = 4$  (d). Parameters of the multiplexed detector are  $M = 10$  and  $\eta = 1$ .

#### IV. ESTIMATION OF MEAN PHOTON NUMBER

The photon number operator  $\hat{n}$  is unbounded. Therefore, without making some additional assumptions, the knowledge of the click statistics  $c_M$  for finite  $M$  does not bound the mean photon number  $\bar{n}$  from above. The reason is that arbitrarily small population of sufficiently large Fock state can increase the mean photon number arbitrarily. For example, if for some fixed  $K$  we have  $p_{K^2} = 1/K$ , then this contributes to the mean photon number by the value  $K^2 p_{K^2} = K$  which can be arbitrarily large for arbitrarily small  $p_{K^2}$ . This effect is illustrated in Fig. 8, where we plot the dependence of the lower and upper bounds on  $\bar{n}$  on the photon number cut-off  $N$ . We can see that the upper bound increases with increasing  $N$  and does not saturate.

Nevertheless, the bound on the mean photon number can be rather tight if we can reliably assume that the contribution of Fock states above some threshold  $N$  is negligible. This could follow for instance from the actual physical mechanism of the state generation. For example, for thermal state with  $\bar{n} = 2$  and detector with  $M = 10$  channels we find that the determination uncertainty  $\Delta\bar{n} < 0.01$  even for the cut-off  $N = 80$ . It is worth noting that the uncertainty of determination of Fock state probabilities is much larger, c.f. Fig. 2(a). For instance  $\Delta p_6 > 0.06$  in this case. However, the possible changes of  $p_n$  with respect to their true values are mutually anti-correlated, since  $p_n$  are constrained by the values of  $c_m$  and by the overall probability normalization. Therefore, the uncertainty of  $\bar{n}$  is much smaller for the cut-off  $N = 80$  than one could naively expect from the uncertainties of  $p_n$ .

To further understand this, we can consider a simple

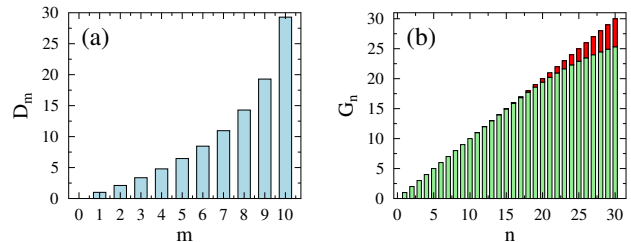


FIG. 9. Example of estimation of the mean photon number  $\bar{n}$  from click statistics,  $M = 10$ ,  $\eta = 1$ . Panel (a) shows a simple estimator  $D$  that is exact for states that do not contain more than 10 photons. In panel (b), this estimator is plotted in the photon number basis (green bars), and the difference between the actual values of the coefficients  $G_n$  and the ideal values  $n$  is indicated by red color.

estimation of the mean photon number

$$\bar{n}_{\text{est}} = \sum_{m=0}^M D_m c_m, \quad (19)$$

which is exact for states containing no more than  $M$  photons. The coefficients  $D_m$  can be determined by solving system of linear equations

$$\sum_{m=0}^M D_m C_{mn} = n, \quad n \leq M. \quad (20)$$

The coefficients  $D_m$  are plotted in Fig. 9(a) for detector with  $M = 10$  channels. The estimator (19) can be also rewritten as

$$\bar{n}_{\text{est}} = \sum_{n=0}^{\infty} G_n p_n, \quad (21)$$

where  $G_n = n$  for  $n \leq M$  and  $G_n < n$  for  $n > M$ . Nevertheless, we find that the performance of the estimator is very good even for several photon numbers above  $M$ , see Fig. 9(b). For example,  $G_{15} = 14.95$ . Asymptotically,  $G_n$  saturate and  $\lim_{n \rightarrow \infty} G_n = D_M$ .

#### V. ANALYTICAL BOUNDS ON SINGLE-PHOTON PROBABILITIES

In this section we provide examples of analytical bounds on single-mode single-photon probability  $p_1$  and the two-mode probability  $p_{1,1}$  that a single photon is present in each mode. These bounds are obtained for simple Hanbury Brown-Twiss setups [35, 36] where two on/off detectors are used to measure each mode. The two-mode probability  $p_{1,1}$  can characterize the probability of successful generation of correlated pair of photons hence its determination is of high practical relevance. Results presented and discussed in this section complement the general numerical analysis performed in the previous

sections. Consider first the single-mode case, where the measured probabilities (3) read  $p_0$  and

$$q_0 = \sum_{n=0}^{\infty} \frac{1}{2^n} p_n. \quad (22)$$

The resulting linear constraints on probabilities  $p_n$  read

$$\sum_{n=1}^{\infty} p_n = 1 - p_0, \quad \sum_{n=1}^{\infty} \frac{1}{2^n} p_n = q_0 - p_0. \quad (23)$$

A lower bound on the single-photon probability  $p_1$  based on knowledge of  $p_0$  and  $q_0$  can be expressed as follows [37, 38]:

$$p_{1,\min} = \max(4q_0 - 3p_0 - 1, 0). \quad (24)$$

Let us first assume that  $4q_0 - 3p_0 - 1 \geq 0$ . The bound (24) is saturated by distribution  $\tilde{p}_0 = p_0$ ,  $\tilde{p}_1 = 4q_0 - 3p_0 - 1$ ,  $\tilde{p}_2 = 2(1 + p_0 - 2q_0)$ , and  $\tilde{p}_n = 0$ ,  $n > 2$ . Using the explicit definition of  $q_0$ , Eq. (22), it is easy to show that  $\tilde{p}_1 \leq p_1$  and  $\tilde{p}_2 \geq 0$ . Explicitly,

$$\tilde{p}_1 = p_1 - \sum_{n=3}^{\infty} \left(1 - \frac{4}{2^n}\right) p_n, \quad \tilde{p}_2 = 2 \sum_{n=2}^{\infty} \left(1 - \frac{2}{2^n}\right) p_n. \quad (25)$$

The lower bound can be equivalently rewritten as

$$p_{1,\min} = y_1(1 - p_0) + y_2(q_0 - p_0), \quad (26)$$

where  $y_1 = -1$  and  $y_2 = 4$ . These coefficients satisfy the inequalities

$$y_1 + \frac{1}{2^n} y_2 \leq \delta_{n1}, \quad n \geq 1. \quad (27)$$

Therefore,  $y_1$  and  $y_2$  represent solution of a linear program that is dual to the minimization of  $p_1$  under the constraints (23). Moreover, a feasible solution of the original linear program exists which saturates the bound (26), as we have just demonstrated above. By duality, this implies the optimality of  $p_{1,\min}$ . Observe that the lower bound  $p_{1,\min} = 4q_0 - 3p_0 - 1$  is tight for all states that do not contain more than two photons, i.e.  $p_n = 0$  for  $n > 2$ .

If  $4q_0 - 3p_0 - 1 < 0$ , then a probability distribution that saturates the bound (24) can be constructed as follows:  $\tilde{p}_0 = p_0$ ,  $\tilde{p}_1 = 0$ ,  $\tilde{p}_2 = 4(q_0 - p_0)$ ,  $p_n = 0$  for  $n > 2$  but finite, and  $\tilde{p}_\infty = 1 + 3p_0 - 4q_0$ . This distribution should be understood as the limit of the sequence of distributions with  $\tilde{p}_n = 0$ ,  $n > 2$ ,  $n \neq N$ , and  $\tilde{p}_N = 1 + 3p_0 - 4q_0$ , when  $N \rightarrow \infty$ . Note that  $\tilde{p}_2 \geq 0$  by construction and also all the constraints (23) are satisfied by construction.

We can also construct an upper bound on  $p_1$ ,

$$p_{1,\max} = 2(q_0 - p_0) = \sum_{n=1}^{\infty} \frac{2}{2^n} p_n. \quad (28)$$

Therefore,  $p_{1,\max} \geq p_1$  by construction. The upper bound (28) is saturated by the following photon number

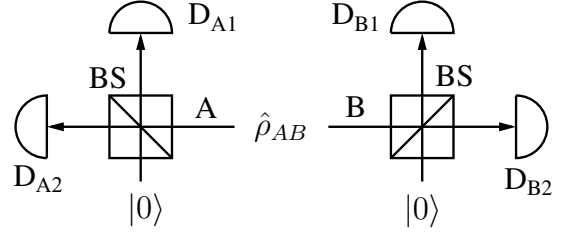


FIG. 10. Hanbury Brown-Twiss type scheme for characterization of single-mode and two-mode states. Each signal mode is split into two halves at a balanced beam splitter BS and each output mode is measured with a binary detector  $D$  that can distinguish the presence and absence of photons. Probabilities of various combinations of clicks or non-clicks of the detectors are measured.

distribution  $\tilde{p}_0 = p_0$ ,  $\tilde{p}_1 = 2(q_0 - p_0)$ ,  $\tilde{p}_\infty = 1 + p_0 - 2q_0$ , and all other  $\tilde{p}_n$  vanish. It follows from Eq. (25) that  $\tilde{p}_\infty \geq 0$  for any true photon number distribution  $p_n$ . This proves the optimality of the upper bound (28).

Let us now consider characterization of the joint photon number distribution  $p_{m,n}$  of a two-mode state  $\hat{\rho}_{AB}$  by local measurements on modes A and B. We assume that each signal is locally split on a balanced beam splitter and each output mode is measured with an on/off detector. By considering only local responses of the detectors observing mode A (or B), we can measure the following probabilities

$$p_{0A} = \sum_{n=0}^{\infty} p_{0,n}, \quad p_{0B} = \sum_{m=0}^{\infty} p_{m,0}, \quad (29)$$

and

$$q_A = \sum_{m,n=0}^{\infty} \frac{1}{2^m} p_{m,n}, \quad q_B = \sum_{m,n=0}^{\infty} \frac{1}{2^n} p_{m,n}. \quad (30)$$

If we consider also the various correlations between non-clicks of detectors that observe modes A and B, we can measure the two-mode vacuum probability  $p_{0,0}$  as well as the probabilities

$$q_{0A} = \sum_{m=0}^{\infty} \frac{1}{2^m} p_{0,m}, \quad q_{0B} = \sum_{n=0}^{\infty} \frac{1}{2^n} p_{n,0}, \quad (31)$$

and

$$q_{00} = \sum_{m,n=0}^{\infty} \frac{1}{2^{m+n}} p_{m,n}. \quad (32)$$

To simplify the subsequent analysis, we will restrict ourselves to symmetric states with  $p_{m,n} = p_{n,m}$  and we will seek bound on  $p_{1,1}$  that reflects this symmetry. We can get rid of all the probabilities  $p_{m,n}$  where  $m = 0$  or  $n = 0$  by constructing the following linear combinations of  $p_{n,m}$ ,

$$D_1 = 1 - p_{0A} - p_{0B} + p_{0,0} = \sum_{m,n=1}^{\infty} p_{m,n}, \quad (33)$$

$$D_2 = q_{00} - q_{0A} - q_{0B} + p_{0,0} = \sum_{m,n=1}^{\infty} \frac{1}{2^{m+n}} p_{m,n}, \quad (34)$$

and

$$D_3 = q_A + q_B - q_{0A} - q_{0B} - p_{0A} - p_{0B} + 2p_{0,0}. \quad (35)$$

We can express  $D_3$  as

$$D_3 = \sum_{m,n=1}^{\infty} \left( \frac{1}{2^m} + \frac{1}{2^n} \right) p_{m,n}. \quad (36)$$

Based on  $D_k$ , a lower bound on  $p_{1,1}$  can be constructed as follows,

$$p_{1,1,\min} = 12D_2 - 2D_3, \quad (37)$$

which is applicable when  $12D_2 - 2D_3 \geq 0$ . A probability distribution that saturates this bound reads  $\tilde{p}_{1,1} = 12D_2 - 2D_3$ ,  $\tilde{p}_{1,2} = \tilde{p}_{2,1} = 2D_3 - 8D_2$ ,  $\tilde{p}_{\infty,\infty} = D_1 + 4D_2 - 2D_3$ , and all other  $\tilde{p}_{m,n}$  with  $m, n \geq 1$  vanish. The meaning of  $\tilde{p}_{\infty,\infty}$  here is the same as the meaning of  $\tilde{p}_{\infty}$  above. Using the explicit expressions for  $D_k$  it is not difficult to check that  $\tilde{p}_{1,2} \geq 0$  and  $\tilde{p}_{\infty,\infty} \geq 0$  for any true distribution  $p_{m,n}$ . Moreover, we have

$$p_{1,1,\min} = \sum_{m,n=1}^{\infty} \left( \frac{12}{2^{m+n}} - \frac{2}{2^m} - \frac{2}{2^n} \right) p_{m,n} \leq p_{1,1}. \quad (38)$$

The inequality in Eq. (38) holds because all the coefficients in front of  $p_{mn}$  in the summation are negative or vanish, except for the coefficient in front of  $p_{1,1}$ , which is equal to 1. Since the inequality (38) can be saturated if  $p_{1,1,\min} \geq 0$ , this proves the optimality of the bound (37) based on knowledge of  $D_k$ . We stress that we have derived the bound assuming symmetry of the photon number distribution. For general states, full information contained in the probabilities (29) - (32) must be utilized to obtain the optimal bound.

## VI. DISCUSSION AND CONCLUSIONS

In summary, we have investigated the fundamental bounds on the ability to determine photon number distribution and other related quantities from tomographically incomplete measurements performed with an array of  $M$  binary detectors which can only distinguish the presence and absence of photons. The measured click statistics generally restricts the values of  $p_n$  to some interval and we have calculated the lower and upper bounds on  $p_n$  by solving appropriate linear programs. We have verified on concrete examples that the precision of determination of the photon number statistics increases with increasing number of detection channels  $M$  and decreases with decreasing detection efficiency  $\eta$ . We have also investigated the determination of parity of the photon number distribution and the estimation of the mean photon number. In our analysis, we have not made any additional

assumptions about the underlying photon number distribution. The proposed approach can be straightforwardly extended to characterization of photon number distributions of multimode fields, although the number of parameters that enter the linear program will rapidly increase with the number of modes.

In our present study, we have deliberately assumed that the true values of the click statistics  $\vec{c} = \{c_m\}$  are known, which allowed us to fully focus on the effects of tomographic incompleteness. In practice, any measurement will be affected by noise due to finite number of samples. The directly measured values  $c_m$  thus can generally differ from the true values and may even be incompatible with any photon number distribution  $p_n$ . Applying statistical approaches, we may try to access the posterior distribution of the physically allowed values of  $c_m$ , determined by the measurement data. If we can sample the posterior distribution of  $\vec{c}$ , we can calculate the effective posterior distribution of each quantity  $Z$  defined by Eq. (5) as follows. For each sample  $\vec{c}_s$ , we find the lower and upper bounds  $z_{\min,s}$  and  $z_{\max,s}$  by solving the linear program (8). After processing  $S$  samples, the posterior distribution of  $Z$  can be approximated by

$$P(z) = \frac{1}{S} \sum_{s=1}^S \frac{1}{\Delta z_s} \chi_{(z_{\min,s}, z_{\max,s})},$$

where  $\chi_{(a,b)}$  is the characteristic function of the interval  $[a, b]$  and  $\Delta z_s = z_{\max,s} - z_{\min,s}$ .

The linear programming approach utilized in this work is applicable to any measurement scheme where the measured probabilities depend linearly on the photon number probabilities and the measurement is tomographically incomplete hence it does not fully determine the distribution  $p_n$ . The matrix coefficients  $C_{mn}$  which connect the photon number statistics  $p_n$  and the measured distribution  $c_m$  are often determined by some theoretical model, but they can be also obtained by quantum measurement tomography [39–47]. Clearly, any uncertainty in the description of the measurement device will further diminish our ability to infer the photon number statistics from the measured data.

The uncertainties of determination of  $p_n$  can be suppressed by using sufficiently large number of detection channels  $M$ . Since increasing the number of detectors may be costly and undesirable, one can break the symmetry of the setup and introduce unbalanced splitting of the signal among the  $M$  detectors. For instance, one can use a sequence of  $M-1$  balanced detectors in the setup in Fig. 1 to achieve effective transmittance  $T_m = 1/2^k$  for  $k$ -th detector, with  $T_{M-1} = T_M$  [48]. The total number of detection channels then increases exponentially with  $M$  because  $2^M - 1$  different transmittances can be probed by measuring the probabilities of non-clicks of each combination of the detectors. However, increasing the number of detection channels will result in increased statistical uncertainty of estimation of each particular click or non-click probability. It may be interesting to investigate the



trade-off between the effect of statistical errors and the tomographic incompleteness, as the effective number of detection channels changes. However, this is beyond the scope of the present paper and we leave it to future work.

## ACKNOWLEDGMENTS

The author acknowledges support by the project OP JAC CZ.02.01.01/00/23\_021/0008790 of the Ministry of

Education, Youth, and Sports of the Czech Republic and EU.

## DATA AVAILABILITY STATEMENT

The data that support the findings of this article will be made openly available on Zenodo.

- 
- [1] A. E. Lita, A. J. Miller, and S. W. Nam, Counting near-infrared single-photons with 95% efficiency, *Opt. Express* **16**, 3032 (2008).
- [2] T. Gerrits, B. Calkins, N. Tomlin, A. E. Lita, A. Migdall, R. Mirin, and S. Woo Nam, Extending single-photon optimized superconducting transition edge sensors beyond the single-photon counting regime, *Opt. Express* **20**, 23798 (2012).
- [3] G. Harder, T. J. Bartley, A. E. Lita, S. Woo Nam, T. Gerrits, and C. Silberhorn, Single-Mode Parametric-Down-Conversion States with 50 Photons as a Source for Mesoscopic Quantum Optics, *Phys. Rev. Lett.* **116**, 143601 (2016).
- [4] J. Sperling, W. R. Clements, A. Eckstein, M. Moore, J. J. Renema, W. S. Kolthammer, S. W. Nam, A. Lita, T. Gerrits, W. Vogel, G. S. Agarwal, and I. A. Walmsley, Detector-Independent Verification of Quantum Light, *Phys. Rev. Lett.* **118**, 163602 (2017).
- [5] O. S. Magaña-Loaiza, Roberto de J. León-Montiel, Armando Perez-Leija, Alfred B. U'Ren, Chenglong You, Kurt Busch, Adriana E. Lita, S. W. Nam, R. P. Mirin, and T. Gerrits, Multiphoton quantum-state engineering using conditional measurements, *Npj Quantum Inf.* **5**, 80 (2019).
- [6] T. Liao, Z. Li, and B. Wang, Direct measurement of the PDC photon statistics by PNR detector, *Opt. Commun.* **477**, 126352 (2020).
- [7] M. Eaton, A. Hossameldin, R. J. Birrittella, P. M. Alsing, C. C. Gerry, H. Dong, C. Cuevas, and O. Pfister, Resolution of 100 photons and quantum generation of unbiased random numbers, *Nat. Photonics* **17**, 106 (2022).
- [8] H. Paul, P. Törmä, T. Kiss, and I. Jex, Photon Chopping: New Way to Measure the Quantum State of Light, *Phys. Rev. Lett.* **76**, 2464 (1996).
- [9] J. Řeháček, Z. Hradil, O. Haderka, J. Peřina, and M. Hamar, Multiple-photon resolving fiber-loop detector, *Phys. Rev. A* **67**, 061801(R) (2003).
- [10] K. Banaszek and I. A. Walmsley, Photon counting with a loop detector, *Opt. Lett.* **28**, 52-54 (2003).
- [11] M. J. Fitch, B. C. Jacobs, T. B. Pittman, and J. D. Franston, Photon-number resolution using time-multiplexed single-photon detectors, *Phys. Rev. A* **68**, 043814 (2003).
- [12] D. Achilles, C. Silberhorn, C. Sliwa, K. Banaszek, and I. A. Walmsley, Fiber-assisted detection with photon number resolution, *Opt. Lett.* **28**, 2387 (2003).
- [13] D. A. Kalashnikov, S. H. Tan, M. Chekhova, and L. A. Krivitsky, Accessing photon bunching with a photon number resolving multi-pixel detector, *Opt. Express* **19**, 9352 (2011).
- [14] J. Sperling, W. Vogel, and G. S. Agarwal, Sub-Binomial Light, *Phys. Rev. Lett.* **109**, 093601 (2012).
- [15] J. Sperling, W. Vogel, and G. S. Agarwal, True photocounting statistics of multiple on-off detectors, *Phys. Rev. A* **85**, 023820 (2012).
- [16] T. J. Bartley, G. Donati, X.-M. Jin, A. Datta, M. Barbieri, and I. A. Walmsley, Direct observation of subbinomial light, *Phys. Rev. Lett.* **110**, 173602 (2013).
- [17] F. Mattioli, Z. Zhou, A. Gaggero, R. Gaudio, R. Leoni, and A. Fiore, Photon-counting and analog operation of a 24-pixel photon number resolving detector based on superconducting nanowires, *Opt. Express* **24**, 9067 (2016).
- [18] J. Kröger, T. Ahrens, J. Sperling, W. Vogel, H. Stolz, and B. Hage, High intensity click statistics from a  $10 \times 10$  avalanche photodiode array, *J. Phys. B: At. Mol. Opt. Phys.* **50**, 214003 (2017).
- [19] D. Zhu, Q.-Y. Zhao, H. Choi, T.-J. Lu, A. E. Dane, D. Englund, and K. K. Berggren, A scalable multiphoton coincidence detector based on superconducting nanowires, *Nat. Nanotechnol.* **13**, 596 (2018).
- [20] I. Straka, L. Lachman, J. Hloušek, M. Miková, M. Mičuda, M. Ježek and R. Filip, Quantum non-Gaussian multiphoton light, *Npj Quantum Inf.* **4**, 4 (2018).
- [21] O. P. Kovalenko, J. Sperling, W. Vogel, and A. A. Semenov, Geometrical picture of photocounting measurements, *Phys. Rev. A* **97**, 023845 (2018).
- [22] J. Tiedau, E. Meyer-Scott, T. Nitsche, S. Barkhofen, T. J. Bartley, and C. Silberhorn, A high dynamic range optical detector for measuring single photons and bright light, *Opt. Express* **27**, 1 (2019).
- [23] L. Lachman, I. Straka, J. Hloušek, M. Ježek, and R. Filip, Faithful Hierarchy of Genuine n-Photon Quantum Non-Gaussian Light, *Phys. Rev. Lett.* **123**, 043601 (2019).
- [24] J. Sperling, A. Eckstein, W. R. Clements, M. Moore, J. J. Renema, W. S. Kolthammer, S. W. Nam, A. Lita, T. Gerrits, I. A. Walmsley, G. S. Agarwal, and W. Vogel, Identification of nonclassical properties of light with multiplexing layouts, *Phys. Rev. A* **96**, 013804 (2017).
- [25] J. Hloušek, M. Dudka, I. Straka, and M. Ježek, Accurate detection of arbitrary photon statistics, *Phys. Rev. Lett.* **123**, 153604 (2019).
- [26] R. Cheng, Y. Zhou, S. Wang, M. Shen, T. Taher, and H. X. Tang, A 100-pixel photon-number-resolving detector unveiling photon statistics, *Nat. Photonics* **17**, 112 (2022).
- [27] J. Hloušek, J. Grygar, M. Dudka, and M. Ježek, High-resolution coincidence counting system for large-scale

- photonics applications, *Phys. Rev. Applied* **21**, 024023 (2024).
- [28] S. Krishnaswamy, F. Schlue, L. Ares, V. Dyachuk, M. Stefszky, B. Brecht, C. Silberhorn, and J. Sperling, Experimental retrieval of photon statistics from click detection, *Phys. Rev. A* **110**, 023717 (2024).
- [29] N. M. Sullivan, B. Braverman, J. Upham and R. W. Boyd, Photon number resolving detection with a single-photon detector and adaptive storage loop, *New J. Phys.* **26**, 043026 (2024).
- [30] T. S. Santana, C. D. Muñoz, R. A. Starkwood, and C. J. Chunnillall, Extending the quantum tomography of a quasi-photon-number-resolving detector, *Opt. Express* **32**, 20350 (2024).
- [31] P. R. Banner, D. Kurdak, Y. Li, A. Migdall, J. V. Porto, and S. L. Rolston, Number-state reconstruction with a single single-photon avalanche detector, *Optica Quantum* **2**, 110 (2024).
- [32] D. Mogilevtsev, Diagonal element inference by direct detection, *Opt. Commun.* **156**, 307 (1998).
- [33] A. R. Rossi, S. Olivares, and M. G. A. Paris, Photon statistics without counting photons, *Phys. Rev. A* **70**, 055801 (2004).
- [34] G. Zambra and M. G. A. Paris, Reconstruction of photon-number distribution using low-performance photon counters, *Phys. Rev. A* **74**, 063830 (2006).
- [35] H. J. Kimble, M. Dagenais, and L. Mandel, Photon antibunching in resonance fluorescence, *Phys. Rev. Lett.* **39**, 691 (1977).
- [36] P. Grangier, G. Roger, and A. Aspect, Experimental evidence for a photon anticorrelation effect on a beam splitter: A new light on single-photon interferences, *Europhys. Lett.* **1**, 173 (1986).
- [37] M. Ježek, I. Straka, M. Mičuda, M. Dušek, J. Fiurášek, and R. Filip, Experimental Test of the Quantum Non-Gaussian Character of a Heralded Single-Photon State, *Phys. Rev. Lett.* **107**, 213602 (2011).
- [38] J. Hloušek, M. Ježek, and J. Fiurášek, Direct Experimental Certification of Quantum Non-Gaussian Character and Wigner Function Negativity of Single-Photon Detectors, *Phys. Rev. Lett.* **126**, 043601 (2021).
- [39] A. Luis and L. L. Sánchez-Soto, Complete Characterization of Arbitrary Quantum Measurement Processes, *Phys. Rev. Lett.* **83**, 3573 (1999).
- [40] J. Fiurášek, Maximum-likelihood estimation of quantum measurement, *Phys. Rev. A* **64**, 024102 (2001).
- [41] J. S. Lundeen, A. Feito, H. Coldenstrodt-Ronge, K. L. Pregnell, Ch. Silberhorn, T. C. Ralph, J. Eisert, M. B. Plenio, and I. A. Walmsley, Tomography of quantum detectors, *Nat. Phys.* **5**, 27 (2009).
- [42] V. D’Auria, N. Lee, T. Amri, C. Fabre, and J. Laurat, Quantum Decoherence of Single-Photon Counters, *Phys. Rev. Lett.* **107**, 050504 (2011).
- [43] G. Brida, L. Ciavarella, I. P. Degiovanni, M. Genovese, L. Lolli, M. G. Mingolla, F. Piacentini, M. Rajteri, E. Taralli, and M. G. A. Paris, Quantum characterization of superconducting photon counters, *New J. Phys.* **14**, 085001 (2012).
- [44] C. M. Natarajan, L. Zhang, H. Coldenstrodt-Ronge, G. Donati, S. N. Dorenbos, V. Zwiller, I. A. Walmsley, and R. H. Hadfield, Quantum detector tomography of a time-multiplexed superconducting nanowire single-photon detector at telecom wavelengths, *Opt. Express* **21**, 893 (2013).
- [45] M. Cooper, M. Karpiński, and B. J. Smith, Local mapping of detector response for reliable quantum state estimation, *Nat. Commun.* **5**, 4332 (2014).
- [46] J. Ma, X. Chen, H. Hu, H. Pan, E. Wu, and H. Zeng, Quantum detector tomography of a single-photon frequency upconversion detection system, *Opt. Express* **24**, 20973 (2016).
- [47] S. Izumi, J. S. Neergaard-Nielsen, and U. L. Andersen, Tomography of a Feedback Measurement with Photon Detection, *Phys. Rev. Lett.* **124**, 070502 (2020).
- [48] J. Fiurášek, Tight nonclassicality criteria for unbalanced Hanbury Brown–Twiss measurement scheme with click detectors, *Phys. Rev. A* **109**, 033713 (2024).